Bilayer Asymmetry Influences Integrin Sequestering in Raft-Mimicking Lipid Mixtures

Noor F. Hussain,[†] Amanda P. Siegel,[†] Yifan Ge,[†] Rainer Jordan,[‡] and Christoph A. Naumann[†*]
[†]Department of Chemistry and Chemical Biology, Indiana University-Purdue University Indianapolis, Indiana; and [‡]Makromolekulare Chemie, Dresden University of Technology, Dresden, Germany

ABSTRACT There is growing recognition that lipid heterogeneities in cellular membranes play an important role in the distribution and functionality of membrane proteins. However, the detection and characterization of such heterogeneities at the cellular level remains challenging. Here we report on the poorly understood relationship between lipid bilayer asymmetry and membrane protein sequestering in raft-mimicking model membrane mixtures using a powerful experimental platform comprised of confocal spectroscopy XY-scan and photon-counting histogram analyses. This experimental approach is utilized to probe the domain-specific sequestering and oligomerization state of $\alpha_v\beta_3$ and $\alpha_5\beta_1$ integrins in bilayers, which contain coexisting liquid-disordered/liquid-ordered (l_d/l_o) phase regions exclusively in the top leaflet of the bilayer (bottom leaflet contains l_d phase). Comparison with previously reported integrin sequestering data in bilayer-spanning l_o-l_d phase separations demonstrates that bilayer asymmetry has a profound influence on $\alpha_v\beta_3$ and $\alpha_5\beta_1$ sequestering behavior. For example, both integrins sequester preferentially to the l_o phase in asymmetric bilayers, but to the l_d phase in their symmetric counterparts. Furthermore, our data show that bilayer asymmetry significantly influences the role of native ligands in integrin sequestering.

INTRODUCTION

The plasma membrane is a complex supramolecular system in which the composition and heterogeneous distribution of lipids in the lipid bilayer matrix may have a profound influence on membrane protein distribution and functionality (1). Lipid rafts prominently reflect the functional importance of lipid heterogeneities, as they have been linked with several important membrane-associated biological processes, including transmembrane (TM) signaling (2), pathogenesis (3), cell adhesion, cell morphology, and angiogenesis (4). These processes are largely associated with the ability of lipid rafts to regulate the sequestration of membrane proteins in the plasma membrane (5). Several molecular processes have been identified as factors determining protein sequestration, including protein acylation, receptor clustering, ligand addition, and other specific protein-protein interactions (6–9). Yet, the underlying factors of protein sequestration and their interaction remain somewhat elusive, largely due to the small size and transient character of raft domains in the plasma membrane (10). Furthermore, common procedures of lipid raft analysis in plasma membranes, such as detergent extraction, cholesterol (CHOL) depletion, and utilization of crosslinking agents, have been shown to be prone to artifacts (11,12).

Therefore, model studies on membrane proteins in well-defined raft-mimicking lipid mixtures with larger size liquid-ordered (l_o)-liquid-disordered (l_d) phase separations have emerged as an attractive complementary tool for the characterization of lipid-raft-associated membrane processes. For example, model membrane experiments confirmed the phase separation of lipids into stable CHOL-rich l_o and CHOL-deficient l_d domains (13,14) and provided insight into the sequestration of membrane proteins in the absence and presence of cross-linking agents in coexisting l_o and l_d domains (15–17). A particularly attractive feature of model membrane experiments is that raft-associated membrane protein sequestering processes can be studied in the absence of artificial cross-linking agents. Recently, our group applied this concept and explored the role of native ligands in integrin sequestering in the presence of raft-mimicking lipid mixtures without artificial cross-linkers (18). To conduct these experiments, we developed a powerful experimental platform comprised of confocal spectroscopy XY-scan, epifluorescence microscopy, and photon-counting histogram (PCH) analyses, in which the sequestration and oligomerization state of TM proteins can be investigated in a planar model membrane system with single-molecule sensitivity. By using this experimental approach, we showed that native ligands alter $\alpha_v\beta_3$ and $\alpha_5\beta_1$ integrin sequestering but not oligomerization in a polymer-tethered lipid bilayer in the presence of bilayer-spanning, coexisting l_o (Bl_o) and l_d (Bl_d) domains. Polymer-tethered membranes were employed because they enable the functional reconstitution of TM proteins (19–21).

In this article, we expand our model membrane experiments on integrins and report on the fascinating but poorly understood relationship between bilayer asymmetry and membrane protein sequestering in raft-mimicking lipid mixtures. It is well established that the plasma membrane of eukaryotic cells is characterized by an asymmetric

Submitted November 27, 2012, and accepted for publication April 9, 2013.

*Correspondence: canauman@iupui.edu

Amanda P. Siegel's present address is Department of Cellular and Integrative Physiology, Indiana University School of Medicine, Indianapolis, IN.

Editor: Paul Wiseman.

0006-3495/13/05/2212/10 $2.00

http://dx.doi.org/10.1016/j.bpj.2013.04.020

distribution of lipids and membrane proteins. One important consequence of the bilayer asymmetry is that sphingolipid- and CHOL-enriched lipid rafts are typically limited to the exoplasmic leaflet of the membrane. At the same time, however, the observed coclustering of raft-associated GPI-anchored proteins in the exoplasmic leaflet and Src-kinase in the cytoplasmic leaflet also suggest a potentially important role of raft domains in transbilayer signaling (22), presumably due to either mediation by TM proteins or a lipid-based transbilayer coupling mechanism (23). To explore the relationship between bilayer asymmetry and integrin sequestering, here we determine the distribution of $\alpha_v\beta_3$ and $\alpha_5\beta_1$ integrins in a polymer-tethered lipid bilayer of asymmetric lipid composition with coexisting l_o-l_d lipid regions and compare these experiments with our previous work on symmetric bilayers (18).

As illustrated in Fig. 1, l_o-l_d phase separations in the asymmetric bilayer system are exclusively located in the top leaflet of the bilayer (bottom leaflet contains a homogeneous l_d phase), whereas those in the symmetric bilayer system exist in both leaflets and are bilayer-spanning. To distinguish monolayer-associated and bilayer-spanning l_o and l_d lipid regions, the following abbreviations are introduced: Ml_o, monolayer-associated l_o region; Ml_d, monolayer-associated l_d region; Bl_o, bilayer-spanning l_o region; and Bl_d, bilayer-spanning l_d region. According to this terminology, the symmetric bilayer exhibits coexisting Bl_o and Bl_d regions, whereas the asymmetric bilayer system shows Ml_o/Ml_d and Bl_d regions. Because the bottom leaflet of the asymmetric bilayer system contains a homogeneous l_d phase, in the following we refer to the lipid mixing behavior in this bilayer system as the coexistence of Ml_o and Bl_d domains. Integrins were chosen because they not only represent important signaling molecules, but are also linked to several raft-associated processes, including cell adhesion, motility, and angiogenesis (24). Polymer-tethered lipid bilayers of asymmetric lipid composition are built layer-by-layer using subsequent Langmuir-Blodgett (LB) and Langmuir-Schaefer (LS) transfers with l_o-l_d phase separating and homogeneous l_d-forming lipid mixtures being in the LS and LB layers, respectively.

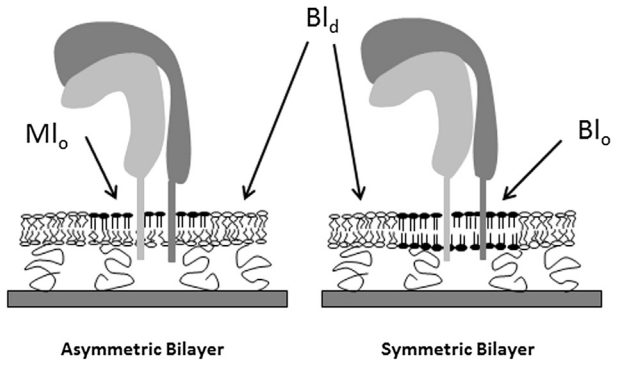

FIGURE 1 Schematic of l_o-l_d phase separations in polymer-tethered lipid bilayers of asymmetric (*left*) and symmetric (*right*) lipid compositions. In the asymmetric bilayer system, l_o-l_d phase separations are exclusively located in the top leaflet (LS monolayer) of the bilayer whereas the bottom leaflet (LB monolayer) is characterized by a homogeneous l_d phase (coexistence between Ml_o and Bl_d regions). In contrast, the symmetric bilayer exhibits bilayer-spanning l_o and l_d regions (coexistence of Bl_o and Bl_d).

A fluorescence-based assay enables the distinction between bilayer-spanning (Bl_o) and monolayer l_o (Ml_o) domains in the planar model membrane system. Importantly, our experiments show that reconstituted $\alpha_v\beta_3$ and $\alpha_5\beta_1$ integrins show a preference for Ml_o domains, which is in marked contrast to the previously observed l_d phase preference in corresponding bilayer systems with coexisting bilayer-spanning l_o (Bl_o) and l_d (Bl_d) regions (18). Furthermore, introduction of reconstituted native ligands ($\alpha_v\beta_3$: vitronectin (VN) and $\alpha_5\beta_1$: fibronectin (FN)) has a different impact on integrin sequestering in lipid mixtures with Ml_o versus Bl_o domains. Corresponding PCH analysis confirms that ligand binding does not alter the integrin oligomerization state. Our findings are significant because they highlight the potentially important role of membrane asymmetry in membrane protein sequestering and function. We hypothesize that bilayer asymmetry in cellular membranes may influence TM protein distribution and functionality in a similar way.

MATERIALS AND METHODS

Materials

The phospholipids DOPC (1,2-dioleoyl-*sn*-glycero-3-phosphocholine), DPPC (1,2-dipalmitoyl-*sn*-glycero-3-phosphocholine), and CHOL were purchased from Avanti Polar Lipids (Alabaster, AL). The procedure for synthesizing the lipopolymer di$C_{18}M_{50}$ (1,2-dioctadecyl-*sn*-glycero-3-*n*-poly(2-methyl-2-oxazoline)$_{50}$) has been described previously in Lüdtke et al. (25). The dye-labeled lipids NBD-DHPE (*n*-(7-nitrobenz-2-oxa-1,3-diazol-4-yl)-1,2-dihexadec-anoyl-*sn*-glycero-3-phosphoethanolamine), TRITC-DHPE (*n*-(6-tetramethylrhodamine-thiocarbamoyl)-1,2-dihexadecanayl-*sn*-glycero-3-phosphoethanolamine, triethylammonium salt), DID (1,1′-dioctadecyl-3,3,3′,3′-tetramethylindodicarbocyanine,4-chlorobenzenesulfonate salt), and DiI (1,1^1-dioctacadecayl-3,3,3^1,3^1-tetramethylindocarbocyanine perchlorate), as well as the kits for fluorescently labeling antibodies with Alexa-555 were obtained from Invitrogen (Carlsbad, CA).

Chloroform (HPLC grade; Fisher Scientific, Pittsburgh, PA) was used as the spreading solvent for the lipid monolayer at the air-water interface in the trough. Milli-Q water (pH = 5.5, 18 MΩ-cm resistivity; Millipore, Billerica, MA) was employed as the subphase material in the trough. Glass coverslips were prepared by first baking them for 3 h at 515°C in a kiln followed by subsequent sonication steps in a bath sonicator using solutions of 1% sodium dodecyl sulfate for 45 min, MeOH saturated with NaOH, and 0.1% HCl (Fisher Scientific). The slides were rinsed with Milli-Q water in between sonication steps for 10 min. Human integrin $\alpha_v\beta_3$ and $\alpha_5\beta_1$, octyl-β-D-glucopyranoside formulation, the monoclonal antibodies (MAbs) anti-integrin $\alpha_v\beta_3$ and anti-integrin $\alpha_5\beta_1$, human purified VN, and human purified FN were purchased from Millipore. Rhodamin6G was obtained from Sigma-Aldrich (St. Louis, MO). The surfactant OG (*n*-octyl-β-D-glucopyranoside) was obtained from Fisher BioReagents (Fairlawn, NJ).

Construction of polymer-tethered phospholipid bilayers containing Ml_o domains

Polymer-tethered phospholipid bilayers of asymmetric lipid composition were prepared layer-by-layer using the LB/LS technique, thereby adapting procedures reported recently for those of symmetric lipid compositions (18,20,26,27). To build the LB and LS monolayers, chloroform solutions of the corresponding lipid/lipopolymer and lipid mixtures were spread at the air-water interface of a film balance with a dipper (Labcon, Darlington, UK). Each monolayer was compressed to 30 mN/m and kept at this pressure for 40 min before monolayer transfer to a glass cover slide. LB monolayer transfers were conducted using the dipper of the film balance. LS transfers were accomplished by positioning a depression slide underneath the air-water interface and gently pushing the cover glass with the LB layer through the LS monolayer onto the depression slide. The depression slide was removed using a transfer dish and the glass substrate with the LB/LS bilayer was transferred to a petri dish, where Milli-Q water was replaced by phosphate-buffered saline (PBS) (Fisher Scientific) 10× concentrations, diluted in Milli-Q water. To obtain a polymer-tethered lipid bilayer without Bl_o domains, but with Ml_o domains in its top leaflet (LS layer), the following LB and LS compositions were employed:

LB layer: (2:1) (DOPC/CHOL) with 5 mol % $diC_{18}M_{50}$; and
LS layer: (1:1:1) (DOPC/DPPC/CHOL).

Alternatively, experiments were conducted with an LS composition of (2.1:1.2:1) (DOPC/DPPC/CHOL). The LS compositions contain 0.4 mol % NBD-DHPE to confirm l_o-l_d phase separations in the asymmetric bilayer system. Furthermore, 0.1 mol % DID, which is less prone to flip-flop, was included in the LB composition to assure that coexisting l_o and l_d phases only form in the top leaflet (LS layer) of the bilayer. To determine the influence of bilayer asymmetry on protein sequestration, experimental findings obtained on the asymmetric bilayer system were compared with those reported on a corresponding symmetric bilayer system (18). In the latter case, the LB and LS compositions were as follows (both monolayers typically contain 0.2 mol % NBD-DHPE):

LB layer: (1:1:1) (DOPC/DPPC/CHOL) with 5 mol % $diC_{18}M_{50}$; and
LS layer: (1:1:1) (DOPC/DPPC/CHOL).

Protein incorporation into bilayers

The incorporation of integrins into polymer-tethered lipid bilayers was accomplished using a modified Rigaud technique (direct protein incorporation method) as described previously in Siegel et al. (18). Briefly, micelle-stabilized membrane proteins (1.3×10^{-11} mol leading to a bilayer concentration of ~10^{-3} mol %) were added to the bilayer sample together with 2 mL of 0.08 mg/mL of OG and incubated for 1.5–2 h. This corresponds to a surfactant concentration in the bilayer sample of ~0.002 critical micelle concentration. To remove the surfactants from the bilayer, a single layer of SM-2 Bio-Beads (Bio-Rad, Hercules, CA) was put on the bilayer sample with the reconstituted integrins for 15 min followed by their removal through extensive rinsing with PBS. Next, Alexa-555 labeled anti-integrin MAbs were added and incubated for 3–4 h at room temperature followed by a washing step with PBS to remove excess antibodies. The MAb labeling strategy is well suited to confirm the functional reconstitution of integrins and to analyze their fluidity, distribution, and oligomerization state in the planar model membrane. Corresponding MAb control experiments on bilayer samples without integrins were conducted to exclude any nonspecific adsorption of antibodies on the bilayer surface. To explore the impact of native ligands on integrin sequestering, VN ($\alpha_v\beta_3$) and FN ($\alpha_5\beta_1$) were added and incubated for 2–4 h at room temperature (1:1 molar ratio of integrin/ligand). Finally, the bilayer was rinsed with PBS to remove excess unbound ligands before imaging.

Microscopy techniques

A confocal ConfoCor 2 system (Carl Zeiss, Jena, Germany) equipped with an Axiovert 200M inverted optical microscope (Carl Zeiss) and C-Apochromat objective (water immersion, 40×, NA = 1.2) was employed to explore the lipid domain-specific distribution and oligomerization state of integrins in the polymer-tethered lipid bilayer using fluorescence fluctuation spectroscopy (FFS) and epifluorescence microscopy (EPI). EPI image acquisition and analysis was done using an AxioCam MRm monochrome digital camera (Carl Zeiss) and Axiovision 4.8 software (Carl Zeiss). EPI was employed to confirm the presence of coexisting l_o and l_d domains in the lipid bilayer. FFS experiments were conducted by confocal spectroscopy XY (CS-XY) scans (maximum scan size: 10 × 10 μm; step size: 0.5 μm) using a 1.0-mW HeNe laser (543 nm) with a 560–615-nm emission filter (the Alexa-555 channel), a 5.0-mW HeNe laser (633 nm) with a 650-nm long-pass filter (the DID channel), and a 30-mW Argon laser (488 nm) with 505–530-nm emission filter (the NBD channel). The 488 and 633 HeNe lasers were utilized to investigate the distribution of the dye lipids NBD-DHPE and DID, respectively. The 543-nm laser was employed to probe the corresponding distribution of Alexa-555-labeled anti-integrin MAbs bound to integrins. Control experiments with DID and NBD-DHPE but without Alexa-555-labeled anti-integrin MAbs were done to correct for background in CS-XY scans.

FFS data were collected in 50-s runs on a bilayer or in a solution to enable fluorescence correlation spectroscopy (FCS) and PCH analysis with the same pinhole size. FCS autocorrelation analysis was used to identify the average brightness of dye-labeled MAbs in solution and to determine the domain-specific lateral mobility of dye-labeled lipids (TRITC-DHPE) in asymmetric and symmetric bilayers with coexisting l_o-l_d regions. Due to uncertainties about the exact shape of the Gaussian intensity profile in the confocal laser spot at the glass-water interface in standard FCS studies, the laser focus dimension, knowledge of the shape of which is required for the determination of diffusion coefficients, was derived by reference to the diffusion coefficient of TRITC-DHPE in a one-component, solid-supported fluid lipid bilayer obtained using the more accurate wide-field single-molecule fluorescence microscopy method described previously (20). The FFS data acquisition for PCH analysis on the bilayer sample was accomplished by maximizing the photon-count rate of laterally mobile, bilayer-based single molecules in the confocal volume.

Data analysis

The domain-specific distribution and oligomerization state of integrins in the presence of Ml_o domains was determined by adapting procedures described by Siegel et al. (18) for coexisting bilayer-spanning l_o and l_d domains. Raw data of the integrin distribution were obtained from confocal XY scans of the NBD-DHPE, DID, and integrin distributions. Each raw data set was corrected for NBD-DHPE and DID channel bleedthrough as well as background. A set of separate experiments showed that the NBD bleedthrough in the Alexa-555 channel represents ~6% of the total background, whereas the DID bleedthrough and background without dye contributions are ~40 and 54%, respectively. To correct for background, control experiments were conducted without integrins and dye-labeled anti-integrin MAbs. Typical signal/background in the presence of integrins with Alexa-555-labeled MAbs was identified to be ~4:1. Bilayers were also constructed with integrins and dye-labeled anti-integrin MAbs with no DID-labeled lipids in the bottom leaflet to determine whether there was an effect on the integrin distribution in the presence of DID lipids. None was evident. The integrin distribution in the bilayer can be quantified in terms of a partition coefficient $K_p(Ml_o/Bl_d)$, defined as I_{Mlo}/I_{Bld}, where I_{Mlo} and I_{Bld} are the intensities from the coexisting Ml_o and Bl_d regions, respectively. The background was subtracted from the intensities obtained from the control experiments without integrins and dye-labeled anti-integrin MAbs. Changes in $K_p(Ml_o/Bl_d)$ can be expressed by the parameter E_{raft}, which is defined as

$$E_{\text{raft}} = \left(\frac{I_{\text{Mlo}} - I_{\text{Bld}}}{I_{\text{Mlo}} + I_{\text{Bld}}}\right). \quad (1)$$

A parameter X_{migrate} can be defined, which provides quantitative information about changes in E_{raft} due to addition of ligands:

$$X_{\text{migrate}} = \left[\frac{E_{\text{raft}(+\text{ligand})} - E_{\text{raft}(-\text{ligand})}}{2}\right]. \quad (2)$$

PCHs of the avalanche photodiode photon counts were used to study the behavior of the oligomerization status of integrins in the bilayer. The PCH method represents a powerful tool to determine the average number and brightness (N_{avg}, ε) of monomers and dimers/multimers of dye-labeled molecules from the analysis of confocal photon count rates (28,29). Using this method, we determined the number and brightness of integrin monomers (N_{avg}, ε) and dimers (N_{avgdimer},$\varepsilon_{\text{dimer}}$ ($=2\varepsilon$)) in the Ml_o and Bl_d phases of the bilayer. These values were used to calculate the mole fraction of the dimers (X_{dimer}) for each species. Corresponding model fits with monomers and tetramers provided comparable results (data not shown). The algorithm that was used to fit the PCH data (the PCH model) was initially tested for its ability to distinguish changes in number and brightness using CdSe/ZnS quantum dots (QDs) in solution and on a bilayer as well as monomeric fluorescent species in solution (Rhodamine 6G and dye-labeled MAbs) and in a planar, glass-supported lipid bilayer (TRITC-DHPE) (data not shown). Previous control experiments on CdSe/ZnS QDs in solution and on a planar, lipid bilayer, which enabled us to calibrate the PCH method for experiments on planar, glass-supported model membranes, showed that the respective QD brightness values are within 5% of each other. The surface modification of CdSe/ZnS QDs and their specific conjugation to lipid bilayers has been described elsewhere (30).

RESULTS AND DISCUSSION

Design and characterization of polymer-tethered lipid bilayers with Ml_o domains

Planar polymer-tethered lipid bilayers with Ml_o domains in their top leaflet were constructed as described in the Materials and Methods. Fig. 2 shows representative EPI micrographs of such a model membrane in which the raftophobic membrane marker DID located exclusively in the bottom leaflet shows a homogeneous distribution whereas the raftophilic membrane marker NBD-DHPE spread in the top leaflet shows distinct evidence of l_o-l_d phase separations:

LS composition: DOPC/DPPC/CHOL (2.1:1.2:1.0) + 0.5 mol % NBD-DHPE; and
LB composition: DOPC/CHOL 2:1 + 5% mol $diC_{18}M_{50}$ + 0.1 mol % DID.

Probe molecules of the DiI family, such as DID, are well suited for this fluorescence assay because their rate of flip-flop is very slow (31), thus providing reliable information about the lipid mixing behavior in the bottom (LB) leaflet of the bilayer. Consequently, in the absence of phase separations in the DID channel, those observed through the NBD channel must be attributed to the presence of Ml_o domains in the top (LS) leaflet of the membrane. (Note: Control experiments on symmetric bilayers with raft-mimicking 1:1:1 DPPC/CHOL/DOPC lipid mixtures confirmed that DID shows preference for the l_d phase in the presence of coexisting l_o and l_d lipid phases; data not shown.) To confirm the stability of Ml_o domains in the polymer-tethered lipid bilayer for membrane protein studies, we conducted EPI microscopy studies on these model membranes over time. Specifically, the stability of the Ml_o domains was confirmed by determining the presence and absence of l_o-l_d phase separations in the NBD and DID channels, respectively, both shortly after construction and 12 h later. To mimic integrin reconstitution conditions, the asymmetric bilayer was incubated in the presence of 0.55 μM OG for 2 h, rinsed, and additionally incubated for 10 h.

As the EPI micrographs of such a bilayer sample in Fig. S1 in the Supporting Material illustrate, the presence and absence of l_o-l_d phase separations through the NBD and DID channels, respectively, assure the feasibility of the experimental assay. Next, we compared the lipid mixing behavior of the asymmetric lipid composition in Fig. 2 with a symmetric lipid composition of (1.5:0.5:1) (DOPC/DPPC/CHOL) (see Fig. S2). The latter represents the scenario of a hypothetical flip-flop-mediated disappearance of DOPC and DPPC concentration gradients across the bilayer. As Fig. S2, *A* and *B*, illustrates, the presence and absence of l_o-l_d phase separations in these asymmetric and symmetric lipid compositions demonstrates the stability of Ml_o domains as employed in this study. Our results are in good agreement with previous findings on model membranes of asymmetric composition with raft-mimicking lipid mixtures, which seem to support a relatively slow spontaneous flip-flop process of phospholipids (26,33).

To characterize l_o-l_d phase separations in asymmetric and symmetric bilayers, we also determined the domain-specific brightness, concentration, and lateral mobility of 0.002 mol % TRITC-DHPE in both types of bilayers using confocal fluorescence intensity and FCS analyses. The results from these lipid domain characterization experiments

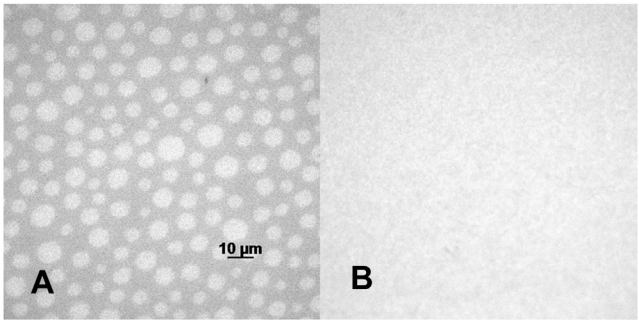

FIGURE 2 EPI-micrographs showing the lipid mixing behavior in the top (*A*) and bottom leaflets (*B*) of the asymmetric lipid bilayer, as observed through the NBD and DiI channels of the microscope. Lipid composition: top (LS) monolayer DOPC/DPPC/CHOL (2.1:1.2:1.0) 0.5 mol % NBD-DHPE; and bottom (LB) monolayer (DOPC/CHOL) 2:1 (5% mol $diC_{18}M_{50}$ and 0.1 mol % DiI).

are summarized in Table 1 together with corresponding control experiments on DOPC, and the binary mixtures DOPC/CHOL (4:1) and DOPC/CHOL (2:1). As Table 1 illustrates, the control experiments show that substantial increases in cholesterol content (lipid packing density) are associated with reduced TRITC-DHPE lateral mobility and brightness. In contrast, the TRITC-DHPE brightness and lateral mobility data determined in asymmetric and symmetric bilayers with monolayer-associated and bilayer-spanning l_o and l_d regions do not show comparable changes, thus excluding substantial differences in lipid packing between both membrane systems. Similarly, domain-specific analysis of the normalized fluorescence intensity, $I = I_{i(i=lo,ld)}/I_{lo} + I_{ld}$, of TRITC-DHPE obtained using CS-XY scans suggests rather moderate lipid-packing differences between monolayer and bilayer-spanning l_o and l_d regions. The observed 47 and 64% reductions (relative to DOPC) of TRITC-DHPE lateral mobility in DOPC/CHOL (4:1) and DOPC/CHOL (2:1), respectively, and the largely indistinguishable lipid lateral mobility of these probe molecules in l_o and l_d regions are in excellent agreement with fluorescence-recovery-after-photobleaching data on comparable lipid mixtures reported recently (34,35).

Integrin sequestration in bilayers with Ml_o domains before and after ligand addition

Integrins were added to a polymer-tethered lipid bilayer containing coexisting Ml_o and Bl_d domains as described in the Materials and Methods, and their domain-specific distribution was determined using confocal CS-XY scans. The methodology has been applied previously to characterize integrins in raft-mimicking lipid mixtures of symmetric composition (Bl_o *and* Bl_d) (18). Fig. 3, *A–J*, compares CS-XY scans of dye-lipid and antibody-labeled integrin ($\alpha_v\beta_3$) distributions in representative bilayer regions of asymmetric and symmetric lipid compositions before (*top row*) and after addition of native ligands (VN) (*bottom row*). In the case of the asymmetric bilayer system, the homogeneous l_d phase in the bottom leaflet and the presence of coexisting l_o-l_d phase separations in the top leaflet of the bilayer are confirmed by the corresponding CS-XY scan data obtained through the DID (*bottom leaflet*, Fig. 3, *A* and *F*) and NBD channels (*top leaflet*, Fig. 3, *B* and *G*). In the symmetric bilayer system, which contains NBD-DHPE in both of its monolayers, bilayer-spanning l_o-l_d phase separations can be observed through the NBD channel (Fig. 3, *D* and *I*). In both types of membrane systems, the corresponding integrin distribution in the same bilayer region is depicted through the Alexa-555 channel (Fig. 3, *C*, *E*, *H*, and *J*)). Examination of the CS-XY scans in Fig. 3 provides valuable qualitative information about the role of bilayer asymmetry on $\alpha_v\beta_3$ sequestration. Specifically, comparison of the NBD and Alexa-555 channel data from both types of bilayer systems provides two intriguing results. Although $\alpha_v\beta_3$ receptors without ligands have a preference for Bl_d regions of the symmetric bilayer (Fig. 3, *D* and *E*, demonstrates opposite preferences), they exhibit a preference for Ml_o regions in the asymmetric bilayer system under comparable ligand-free conditions (Fig. 3, *B* and *C*, shows similar preferences). Furthermore, addition of native ligands (VN) has a different impact on integrin distribution in both types of bilayers, as exemplified by the observed ligand-mediated $\alpha_v\beta_3$ net translocation from Bl_d to Bl_o regions in symmetric bilayers (Fig. 3, *D* and *E*, versus Fig. 3, *I* and *J*) and the largely unchanged Ml_o affinity in their asymmetric counterparts (Fig. 3, *B* and *C*, versus Fig. 3, *G* and *H*). Comparable qualitative results were obtained from corresponding CS-XY scans of $\alpha_5\beta_1$ integrin (data not shown).

As outlined in the Materials and Methods, the CS-XY data can be analyzed in terms of the parameter E_{raft}, which provides a quantitative measure of protein sequestering in the planar model membrane environment. Fig. 4 summarizes the E_{raft} values of $\alpha_v\beta_3$ and $\alpha_5\beta_1$ obtained in the presence of coexisting Ml_o and Bl_d domains together with corresponding E_{raft} data on bilayer systems with coexisting bilayer-spanning Bl_o and Bl_d domains, reported recently in Siegel et al. (18). Most notably, in the absence of native ligands, the E_{raft} data of $\alpha_v\beta_3$ and $\alpha_5\beta_1$ illustrate a

TABLE 1 Characterization of l_o-l_d phase separations in asymmetric and symmetric bilayers

Bilayer type	Diffusion time (ms)	Diffusion coefficient ($\mu m^2/s$)	Brightness (PCH analysis)	Normalized fluorescence intensity (CS-XY analysis)
DOPC only	3.16 ± 0.34	1.68 ± 0.20	6.25 ± 0.71	—
DOPC:CHOL (4:1)	5.89 ± 0.99	0.89 ± 0.15	4.57 ± 0.79	—
DOPC:CHOL (2:1)	8.69 ± 1.50	0.61 ± 0.13	3.45 ± 0.36	—
Asymmetric-l_d (Bl_d)	5.87 ± 1.65	0.90 ± 0.21	3.97 ± 0.57	0.60 ± 0.03
Asymmetric-l_o (Ml_o)	6.19 ± 1.17	0.86 ± 0.15	3.77 ± 0.73	0.40 ± 0.02
Symmetric-l_d (Bl_d)	6.21 ± 1.17	0.90 ± 0.14	4.10 ± 0.40	0.70 ± 0.03
Symmetric-l_o (Bl_o)	6.34 ± 1.34	0.83 ± 0.15	3.57 ± 0.44	0.30 ± 0.02

FCS analysis provides information about the lateral mobility (diffusion time and diffusion coefficient) of TRITC-DHPE in the different lipid environments. PCH analysis gives complementary insight into the average brightness per TRITC-DHPE molecule. The normalized fluorescence intensity values, $I = I_i(i = l_o,l_d)/I_{lo} + I_{ld}$, obtained using CS-XY scans were corrected for background and CHOL-induced intensity changes (determined by PCH-based TRITC-DHPE brightness analysis). Together, the different data in Table 1 indicate that there are no substantial differences in lipid packing between l_o-l_d regions in both types of bilayer systems.

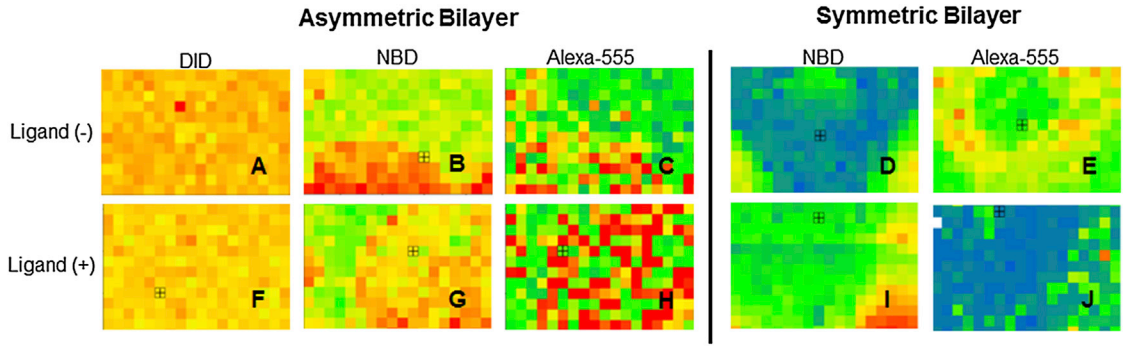

FIGURE 3 Representative CS-XY scans of $\alpha_v\beta_3$ integrin distribution in the presence of monolayer-associated (asymmetric bilayer) and bilayer-spanning (symmetric bilayer) l_o-l_d phase separations before (*top row*) and after addition of VN (*bottom row*). In the asymmetric system, the presence of monolayer-associated l_o and l_d regions is confirmed by the CS-XY data through the DID (*A* and *F*) and NBD (*B* and *G*) channels, whereas the corresponding integrin distribution is determined by the Alexa-555 channel (*C* and *H*). In the symmetric system, lipid phase separations and corresponding integrin distribution are identified through the NBD (*D* and *I*) and Alexa-555 channels (*E* and *J*), respectively. Box $= 6 \times 9\ \mu m^2$.

moderately higher affinity for the Ml_o over coexisting Bl_d domains. In contrast, these integrins exhibit a preference for the Bl_d-phase in the symmetric bilayer system (18). A comparison of integrin affinity data from both types of membrane compositions sets a hierarchy: Ml_o is the preferred state, followed by Bl_d, followed by Bl_o.

Several partially competing factors are known to contribute to the specific lipid domain affinity of membrane proteins (36), the three most important of which are bilayer compressibility, bilayer width, and interactions between the extracellular integrin headgroup and the bilayer itself. The l_d phase preference of TM α-helical structures of membrane proteins is considered as one important factor of protein sequestering in heterogeneous lipid environments that can be related to bilayer compressibility. For example, it has been shown that α-helices of TM domains, when constructed as simple peptides, associate strongly with l_d regions (37). This l_d phase preference of TM domains can be rationalized in terms of differences in bilayer compressibility modulus (lipid-packing density) in l_d and l_o domains, which affects the energy to incorporate membrane proteins into the lipid bilayer (36).

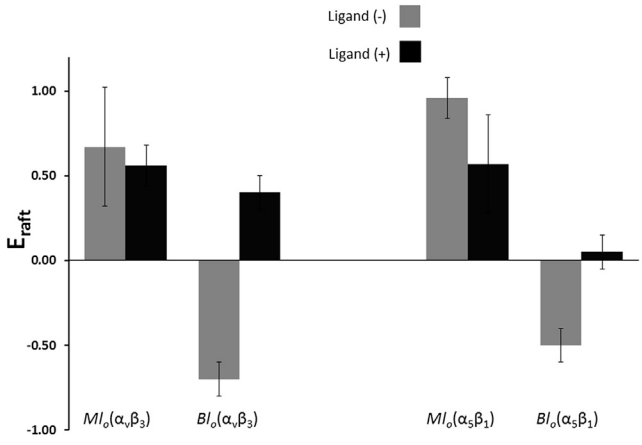

FIGURE 4 Comparison of E_{raft} values for $\alpha_v\beta_3$ and $\alpha_5\beta_1$ (with and without integrin ligands) as determined for bilayers with Ml_o and Bl_o domains (*light bars*, −ligand; *dark bars*, +ligand).

E_{raft} analysis of dye-labeled lipids provides some insight into lipid-packing conditions in monolayer-associated and bilayer-spanning l_o-l_d regions:

1. TRITC-DHPE distribution in the presence of coexisting l_o-l_d regions in asymmetric and symmetric bilayers provides E_{raft} values of −0.2 and −0.46, respectively. These E_{raft} data of TRITC-DHPE suggest that the Ml_o phase has a slightly lower lipid-packing density and greater compressibility than the Bl_o phase. In other words, the observed Ml_o phase preference of integrins in asymmetric bilayer systems can be rationalized, at least in part, in terms of the more favorable energetics of protein incorporation in these membrane regions relative to their bilayer-spanning counterparts.
2. Hydrophobic matching of protein TM and bilayer hydrophobic regions represents another significant factor that determines the affinity of membrane proteins for particular lipid environments. Previously reported bilayer x-ray diffraction data of DOPC-CHOL and CHOL-sphingolipid mixtures, and DOPC indicate hydrophobic thicknesses values of the bilayer for the Bl_d, Ml_o, and Bl_o domains of ~33 ± 1 Å (Bl_d), 35.5 ± 1 Å (Ml_o), and 38 ± 1 Å (Bl_o) (38). Interestingly, the hydrophobic thickness value of Bl_d domains best matches those reported for TM α-helices of integrin α- and β-subunits, which are 31.6 ± 3.4 Å and 30.0 ± 3.6 Å, respectively (39,40). Therefore, the previously reported l_d-phase preference of $\alpha_v\beta_3$ and $\alpha_5\beta_1$ in the presence of coexisting Bl_d and Bl_o domains in the symmetric bilayer compositions appears plausible on the basis of hydrophobic matching arguments (available hydrophobic thickness data), as a hypothetical l_o phase association of integrins would be accompanied by a substantial hydrophobic thickness mismatch of ~7 Å.

3. The situation is less obvious in the asymmetric membrane system because the reported error margin of the integrin hydrophobic thickness of ~3.5 Å does not exclude a scenario of similar hydrophobic mismatch conditions in Ml_o and Bl_d membrane regions. Therefore, the observed Ml_o phase preference in asymmetric bilayers with coexisting Ml_o and Bl_d domains may indicate contributions from another regulatory factor affecting protein affinity for lipid domains. This third factor is most likely linked to the interaction between the lipid bilayer and the extracellular integrin headgroups or ectodomains. Indeed, contributions from ectodomain-lipid interactions can be expected if one considers the close vicinity of bent ectodomains and lipid bilayer in resting, inactive integrins. The observed hierarchical preferences suggest that these interactions lead to a moderate l_o phase preference in asymmetric, raft-mimicking lipid compositions. Interestingly, a comparison of integrin E_{raft} data without ligands in Fig. 4 shows a slightly higher l_o phase preference of $\alpha_5\beta_1$ relative to $\alpha_v\beta_3$. This enhanced l_o phase preference, which suggests subtle differences in lipid-protein interactions, can be observed for both symmetric and asymmetric lipid compositions.
4. The next significant finding from Fig. 4 is the relatively minor change in integrin sequestering upon addition of ligands in the asymmetric bilayer systems, which is in stark contrast to the substantial translocation from Bl_d to Bl_o phases in symmetric bilayer systems. For $\alpha_v\beta_3$, in the Ml_o system, there was very little change in raftophilicity ($X_{\mathrm{migrate}}(\alpha_v\beta_3) = -5.5 \pm 6\%$), whereas in the Bl_o system more than half of the proteins translocated from Bl_d to Bl_o domains (18). This difference becomes understandable if one considers the reported large change in integrin ectodomain orientation that has been reported to occur upon the addition of the extracellular ligands and cytosolic integrin-binding proteins (41,42). The conformation becomes more stretched upon ligand binding, and this change is accompanied by a substantial reorganization of the TM α-helical structures and cytosolic domains of the α- and β-subunits, including a change in the tilt angle. For example, fluorescence resonance energy transfer experiments on integrins in the plasma membrane have shown that ligand-mediated conformational changes of integrin ectodomains can be propagated across the plasma membrane, thereby leading to a significant separation of α- and β-integrin tails (43). Furthermore, multiscale simulations on integrin $\alpha_{\mathrm{IIb}}/\beta_3$ TM helix dimer in the presence of a POPC/POPG lipid bilayer showed that α_{IIb} mutations, which were found to have a significant effect on integrin activation (44), lead to a perturbation of TM helix packing and changing crossing angles of the two integrin TM helices from 35° (wild-type) to 10° (mutation) (45). Interestingly, upon integrin activation, the tilt angle of β_3 remained largely constant at 30°, whereas that of α_{IIb} changed from 5° to 20°. Based on these structural data, one can expect that ligand binding to $\alpha_v\beta_3$ and $\alpha_5\beta_1$ leads to a rather stretched conformation of integrin ectodomains, which should reduce the interactions between ectodomain and lipid bilayer. Furthermore, we hypothesize that the quite reproducible l_o phase preference upon ligand binding in symmetric and asymmetric bilayer compositions can be attributed to the parallel reorganization of the integrin TM region, which includes the opening up of the tight association and the tilting of the two integrin TM helices in the Bl_d phase region.

PCH analysis to determine degree of integrin oligomerization

Ligands and crosslinking agents are known to alter the sequestering of membrane proteins in coexisting l_d and l_o lipid phases (46,47). Therefore, we next determined the oligomerization state of $\alpha_v\beta_3$ and $\alpha_5\beta_1$ in Ml_o-containing bilayers with and without their respective ligands using PCH analysis. As reported before for integrins in bilayers with bilayer-spanning l_d and l_o lipid domains, the PCH data were analyzed in terms of a model, which provides insight into the domain-specific number and brightness of integrin monomers (N_{avg}, ε) and dimers (N_{avgdimer},$\varepsilon_{\mathrm{dimer}}$ (= 2ε)) (18). Fig. 5 summarizes the results of the PCH analysis of $\alpha_v\beta_3$ and $\alpha_5\beta_1$ in bilayers with coexisting Ml_o and Bl_d domains. It includes experimentally determined PCH curves (*markers*) and best model fits (*dashed line*) (Fig. 5, *A–D*), as well as the results of the PCH model-derived molecular brightness, ε (Fig. 5 *E*), and fraction of dimers, X_{dimer} (Fig. 5 *F*). Fig. 5 *E* shows that the ratio of ε of Alexa-555 labeled anti-integrin MAbs bound to bilayer-incorporated integrins and in solution remains in the range of 83 ± 1% regardless of the addition of ligands.

This is in excellent agreement with our previous findings on integrins in bilayers with bilayer-spanning l_o-l_d phase separations (18). Fig. 5 *F* suggests that $\alpha_v\beta_3$ and $\alpha_5\beta_1$ in the lipid bilayer primarily exist as monomers with and without VN and FN, respectively, again in good agreement with recent results on bilayers with membrane-spanning domains (18). The results in Fig. 5, *E* and *F*, are significant because they imply that ligand addition does not cause any significant integrin oligomerization in the model membrane environment. These model membrane results are mirrored by comparable findings on integrins in OG-containing solution (48) and in plasma membranes in the absence of cytosolic integrin linkages (49). In the first case, any notable ligand-mediated integrin oligomerization could be excluded because the molecular weight of integrins determined by centrifugation remained within 10% the same before and after ligand addition. In the second case,

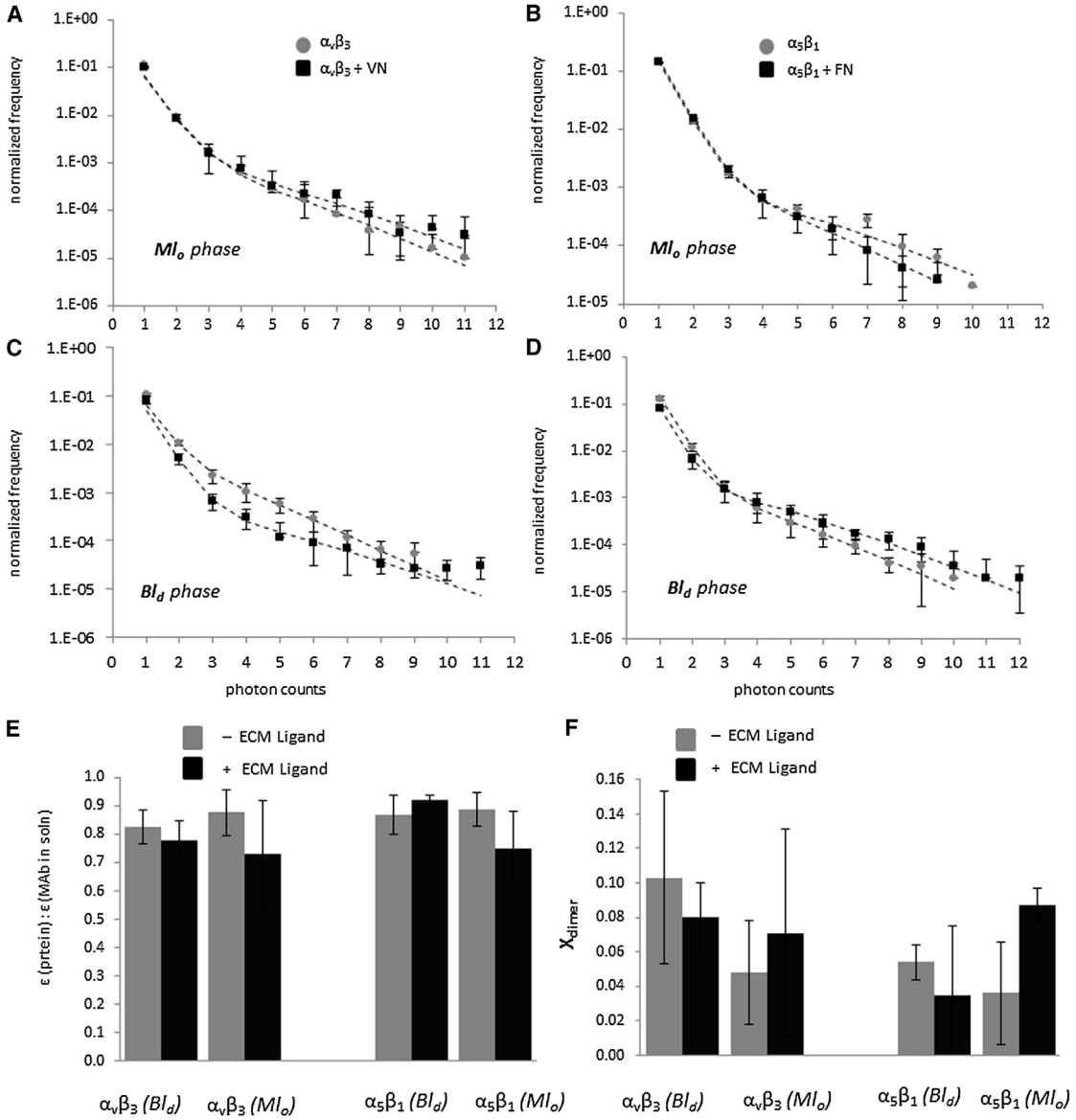

FIGURE 5 PCH curves for $\alpha_v\beta_3$ (*A* and *C*) and $\alpha_5\beta_1$ (*B* and *D*) before (*light markers*) and after (*dark markers*) ligand binding in both l_o phase (*A* and *B*) and l_d phase (*C* and *D*). (*Dotted lines*) Best-fit curves from PCH algorithm. (*E*) Brightness compared to MAbs in solution and (*F*) fraction of dimers found through PCH analysis of $\alpha_v\beta_3$ (*left*) and $\alpha_5\beta_1$ (*right*) integrin proteins before (*light bars*) and after (*dark bars*) ligand binding in l_d and l_o phases.

no integrin clustering was observed after ligand addition to integrins without cytosolic linkage.

CONCLUSION

This work provides direct experimental evidence that bilayer asymmetry has a significant impact on the sequestering of integrins in raft-mimicking lipid mixtures. Unlike in bilayers with bilayer-spanning l_o and l_d lipid phases, $\alpha_v\beta_3$ and $\alpha_5\beta_1$ integrins are deficient in Bl_d domains of bilayers, in which l_o and l_d phase separations are limited to the top leaflet of the bilayer. Moreover, comparing CS-XY and PCH experiments on these integrins in bilayers with Ml_o versus Bl_o domains in the absence and presence of their respective ligands demonstrate the different influence of ligand binding on integrin sequestering in bilayers of symmetric and asymmetric lipid compositions. The observed l_d and l_o phase preferences of $\alpha_v\beta_3$ and $\alpha_5\beta_1$ in bilayers with Bl_o and Ml_o domains suggests two potential mechanisms of integrin sequestering regulation—predominantly sequestration regulation by changing hydrophobic matching conditions and, to a lesser extent, sequestration regulation by alterations in lipid composition affecting lipid packing.

The detected changes of integrin sequestering after ligand addition are likely associated with distinct ligand-induced conformational changes of integrins influencing hydrophobic matching and integrin-lipid interactions. Our experimental results are significant because they highlight the

potential importance of bilayer asymmetry in protein sequestering and function in biological membranes. They support a mechanism of protein sequestration, which is based on the subtle interplay of different molecular interactions. Our findings are particularly exciting in light of the postulated functional importance of some TM proteins in the assembly of raft-mediated transbilayer platforms (50–52). They are also intriguing with regard to recent findings that $\alpha_5\beta_1$ seems to recruit CHOL to the exoplasmic leaflet of plasma membranes (53). Furthermore, the observed ability of integrins to affiliate with the l_o phase is interesting if one considers that several integrin-related cellular processes, such as cell adhesion, migration, and angiogenesis, are considered raft-associated (46,47,54,55). Importantly, the described methodology, which enables the parallel analysis of membrane protein sequestering and oligomerization under well-defined conditions with single-molecule sensitivity, can be conducted in the absence of artificial crosslinking agents. In that sense, it provides valuable complementary information to corresponding protein sequestering studies at the cellular level.

SUPPORTING MATERIAL

Two figures are available at http://www.biophysj.org/biophysj/supplemental/S0006-3495(13)00453-0.

This work was supported in part by the National Science Foundation (grant No. MCB-0920134) and the Indiana University-Purdue University Indianapolis Nanoscale Imaging Center.

REFERENCES

1. Edidin, M. 2001. Shrinking patches and slippery rafts: scales of domains in the plasma membrane. *Trends Cell Biol.* 11:492–496.
2. Holowka, D., J. A. Gosse, …, B. Baird. 2005. Lipid segregation and IgE receptor signaling: a decade of progress. *Biochim. Biophys. Acta.* 1746:252–259.
3. Pelkmans, L. 2005. Secrets of caveolae- and lipid raft-mediated endocytosis revealed by mammalian viruses. *Biochim. Biophys. Acta.* 1746:295–304.
4. Carman, C. V., and T. A. Springer. 2003. Integrin avidity regulation: are changes in affinity and conformation underemphasized? *Curr. Opin. Cell Biol.* 15:547–556.
5. Brown, D. A., and E. London. 1998. Functions of lipid rafts in biological membranes. *Annu. Rev. Cell Dev. Biol.* 14:111–136.
6. Zacharias, D. A., J. D. Violin, …, R. Y. Tsien. 2002. Partitioning of lipid-modified monomeric GFPs into membrane microdomains of live cells. *Science.* 296:913–916.
7. Gulbins, E., and H. Grassmé. 2002. Ceramide and cell death receptor clustering. *Biochim. Biophys. Acta.* 1585:139–145.
8. Fallahi-Sichani, M., and J. J. Linderman. 2009. Lipid raft-mediated regulation of G-protein coupled receptor signaling by ligands which influence receptor dimerization: a computational study. *PLoS ONE.* 4:e6604.
9. Kimura, A., C. A. Baumann, …, A. R. Saltiel. 2001. The sorbin homology domain: a motif for the targeting of proteins to lipid rafts. *Proc. Natl. Acad. Sci. USA.* 98:9098–9103.
10. Stöckl, M. T., and A. Herrmann. 2010. Detection of lipid domains in model and cell membranes by fluorescence lifetime imaging microscopy. *Biochim. Biophys. Acta.* 1798:1444–1456.
11. Ganguly, S., and A. Chattopadhyay. 2010. Cholesterol depletion mimics the effect of cytoskeletal destabilization on membrane dynamics of the serotonin 1A receptor: a zFCS study. *Biophys. J.* 99:1397–1407.
12. Lichtenberg, D., F. M. Goñi, and H. Heerklotz. 2005. Detergent-resistant membranes should not be identified with membrane rafts. *Trends Biochem. Sci.* 30:430–436.
13. Dietrich, C., L. A. Bagatolli, …, E. Gratton. 2001. Lipid rafts reconstituted in model membranes. *Biophys. J.* 80:1417–1428.
14. Kaiser, H. J., D. Lingwood, …, K. Simons. 2009. Order of lipid phases in model and plasma membranes. *Proc. Natl. Acad. Sci. USA.* 106:16645–16650.
15. Baumgart, T., A. T. Hammond, …, W. W. Webb. 2007. Large-scale fluid/fluid phase separation of proteins and lipids in giant plasma membrane vesicles. *Proc. Natl. Acad. Sci. USA.* 104:3165–3170.
16. Kahya, N., D. A. Brown, and P. Schwille. 2005. Raft partitioning and dynamic behavior of human placental alkaline phosphatase in giant unilamellar vesicles. *Biochemistry.* 44:7479–7489.
17. Sengupta, P., A. Hammond, …, B. Baird. 2008. Structural determinants for partitioning of lipids and proteins between coexisting fluid phases in giant plasma membrane vesicles. *Biochim. Biophys. Acta.* 1778:20–32.
18. Siegel, A. P., A. Kimble-Hill, …, C. A. Naumann. 2011. Native ligands change integrin sequestering but not oligomerization in raft-mimicking lipid mixtures. *Biophys. J.* 101:1642–1650.
19. Wagner, M. L., and L. K. Tamm. 2000. Tethered polymer-supported planar lipid bilayers for reconstitution of integral membrane proteins: silane-polyethyleneglycol-lipid as a cushion and covalent linker. *Biophys. J.* 79:1400–1414.
20. Deverall, M. A., E. Gindl, …, C. A. Naumann. 2005. Membrane lateral mobility obstructed by polymer-tethered lipids studied at the single molecule level. *Biophys. J.* 88:1875–1886.
21. Purrucker, O., S. Gonnenwein, …, M. Tanaka. 2007. Polymer-tethered membranes as quantitative models for the study of integrin-mediated cell adhesion. *Soft Matter.* 3:333–336.
22. Harder, T., P. Scheiffele, …, K. Simons. 1998. Lipid domain structure of the plasma membrane revealed by patching of membrane components. *J. Cell Biol.* 141:929–942.
23. Kusumi, A., I. Koyama-Honda, and K. Suzuki. 2004. Molecular dynamics and interactions for creation of stimulation-induced stabilized rafts from small unstable steady-state rafts. *Traffic.* 5:213–230.
24. Gaus, K., S. Le Lay, …, M. A. Schwartz. 2006. Integrin-mediated adhesion regulates membrane order. *J. Cell Biol.* 174:725–734.
25. Lüdtke, K., R. Jordan, …, C. A. Naumann. 2005. Lipopolymers from new 2-substituted-2-oxazoline for artificial cell membrane constructs. *Macromol. Biosci.* 5:384–393.
26. Garg, S., J. Rühe, …, C. A. Naumann. 2007. Domain registration in raft-mimicking lipid mixtures studied using polymer-tethered lipid bilayers. *Biophys. J.* 92:1263–1270.
27. Naumann, C. A., O. Prucker, …, C. W. Frank. 2002. The polymer-supported phospholipid bilayer: tethering as a new approach to substrate-membrane stabilization. *Biomacromolecules.* 3:27–35.
28. Chen, Y., J. D. Müller, …, E. Gratton. 1999. The photon counting histogram in fluorescence fluctuation spectroscopy. *Biophys. J.* 77:553–567.
29. Huang, B., T. D. Perroud, and R. N. Zare. 2004. Photon counting histogram: one-photon excitation. *ChemPhysChem.* 5:1523–1531.
30. Murcia, M. J., D. E. Minner, …, C. A. Naumann. 2008. Design of quantum dot-conjugated lipids for long-term, high-speed tracking experiments on cell surfaces. *J. Am. Chem. Soc.* 130:15054–15062.
31. Wolf, D. E. 1985. Determination of the sidedness of carbocyanine dye labeling of membranes. *Biochemistry.* 24:582–586.

32. Reference deleted in proof.

33. Crane, J. M., V. Kiessling, and L. K. Tamm. 2005. Measuring lipid asymmetry in planar supported bilayers by fluorescence interference contrast microscopy. *Langmuir.* 21:1377–1388.

34. Crane, J. M., and L. K. Tamm. 2004. Role of cholesterol in the formation and nature of lipid rafts in planar and spherical model membranes. *Biophys. J.* 86:2965–2979.

35. Kiessling, V., and L. K. Tamm. 2006. Transbilayer effects of raft-like lipid domains in asymmetric planar bilayers measured by single molecule tracking. *Biophys. J.* 91:3313–3326.

36. McIntosh, T. J., and S. A. Simon. 2006. Roles of bilayer material properties in function and distribution of membrane proteins. *Annu. Rev. Biophys. Biomol. Struct.* 35:177–198.

37. Fastenberg, M. E., H. Shogomori, …, E. London. 2003. Exclusion of a transmembrane-type peptide from ordered-lipid domains (rafts) detected by fluorescence quenching: extension of quenching analysis to account for the effects of domain size and domain boundaries. *Biochemistry.* 42:12376–12390.

38. Gandhavadi, M., D. Allende, …, T. J. McIntosh. 2002. Structure, composition, and peptide binding properties of detergent soluble bilayers and detergent resistant rafts. *Biophys. J.* 82:1469–1482.

39. Lomize, A., M. Lomize, and I. Pogozheva. 2005–2011. Membranome Database—Human Membrane Atlas (Integrin α-V). College of Pharmacy, University of Michigan, Ann Arbor, MI.

40. Lomize, A., M. Lomize, and I. Pogozheva. 2005–2011. Orientations of Proteins in Membranes (OPM) Database (Integrin β-3, Transmembrane Helix). Mosberg Lab, College of Pharmacy, University of Michigan, Ann Arbor, MI.

41. Shattil, S. J., C. Kim, and M. H. Ginsberg. 2010. The final steps of integrin activation: the end game. *Nat. Rev. Mol. Cell Biol.* 11:288–300.

42. Du, X. P., E. F. Plow, …, M. H. Ginsberg. 1991. Ligands "activate" integrin αIIb β3 (platelet GPIIb-IIIa). *Cell.* 65:409–416.

43. Kim, M., C. V. Carman, and T. A. Springer. 2003. Bidirectional transmembrane signaling by cytoplasmic domain separation in integrins. *Science.* 301:1720–1725.

44. Hughes, P. E., F. Diaz-Gonzalez, …, M. H. Ginsberg. 1996. Breaking the integrin hinge. A defined structural constraint regulates integrin signaling. *J. Biol. Chem.* 271:6571–6574.

45. Kalli, A. C., I. D. Campbell, and M. S. P. Sansom. 2011. Multiscale simulations suggest a mechanism for integrin inside-out activation. *Proc. Natl. Acad. Sci. USA.* 108:11890–11895.

46. Cunningham, O., A. Andolfo, …, N. Sidenius. 2003. Dimerization controls the lipid raft partitioning of uPAR/CD87 and regulates its biological functions. *EMBO J.* 22:5994–6003.

47. Wong, S. W., M. J. Kwon, …, D. H. Hwang. 2009. Fatty acids modulate Toll-like receptor 4 activation through regulation of receptor dimerization and recruitment into lipid rafts in a reactive oxygen species-dependent manner. *J. Biol. Chem.* 284:27384–27392.

48. Hantgan, R. R., C. Paumi, …, J. W. Weisel. 1999. Effects of ligand-mimetic peptides Arg-Gly-Asp-X (X = Phe, Trp, Ser) on αIIbβ3 integrin conformation and oligomerization. *Biochemistry.* 38:14461–14474.

49. Takagi, J., K. Strokovich, …, T. Walz. 2003. Structure of integrin $\alpha_5\beta_1$ in complex with fibronectin. *EMBO J.* 22:4607–4615.

50. Brückner, K., J. Pablo Labrador, …, R. Klein. 1999. Ephrin-B ligands recruit GRIP family PDZ adaptor proteins into raft membrane microdomains. *Neuron.* 22:511–524.

51. Sebald, A., I. Mattioli, and M. L. Schmitz. 2005. T-cell receptor-induced lipid raft recruitment of the IκB kinase complex is necessary and sufficient for NF-κB activation occurring in the cytosol. *Eur. J. Immunol.* 35:318–325.

52. Huber, T. B., B. Schermer, …, T. Benzing. 2006. Podocin and MEC-2 bind cholesterol to regulate the activity of associated ion channels. *Proc. Natl. Acad. Sci. USA.* 103:17079–17086.

53. Pankov, R., T. Markovska, …, A. Momchilova. 2005. Cholesterol distribution in plasma membranes of β1 integrin-expressing and β1 integrin-deficient fibroblasts. *Arch. Biochem. Biophys.* 442:160–168.

54. Blystone, S. D., I. L. Graham, …, E. J. Brown. 1994. Integrin αvβ3 differentially regulates adhesive and phagocytic functions of the fibronectin receptor α5β1. *J. Cell Biol.* 127:1129–1137.

55. Kalvodova, L., N. Kahya, …, K. Simons. 2005. Lipids as modulators of proteolytic activity of BACE: involvement of cholesterol, glycosphingolipids, and anionic phospholipids in vitro. *J. Biol. Chem.* 280:36815–36823.

Bilayer Asymmetry Influences Integrin Sequestering in Raft-Mimicking Lipid Mixtures

Noor F. Hussain[†], Amanda P. Siegel[†] , Yifan Ge[†], Rainer Jordan[‡], Christoph A. Naumann[†,*]

[†] Department of Chemistry and Chemical Biology, Indiana University-Purdue University Indianapolis, Indiana; and [‡] Makromolekulare Chemie, TU Dresden, Dresden, Germany.

Supporting Materials

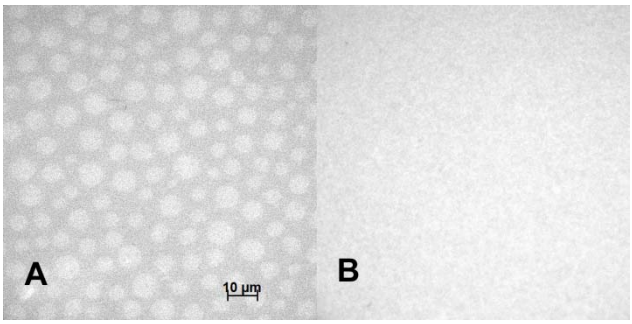

Figure S1: EPI-micrographs illustrating the lipid mixing behavior in the top (A) and bottom leaflets (B) of the asymmetric lipid bilayer 12 h after bilayer preparation. To mimic integrin reconstitution conditions, this bilayer was incubated in 0.55µM OG for 2 hrs followed by washing with PBS buffer [lipid composition: top (LS) monolayer –DOPC: DPPC: CHOL- (2.1: 1.2: 1.0) 0.5mol% NBD-DHPE; bottom (LB) monolayer - (DOPC: CHOL) -2:1 (5% mol $diC_{18}M_{50}$ & 0.1mol% DiI)].

*Correspondence: canauman@iupui.edu
Amanda P. Siegel's present address is Dept. Cellular and Integrative Physiology, Indiana University School of Medicine, Indianapolis, Indiana.

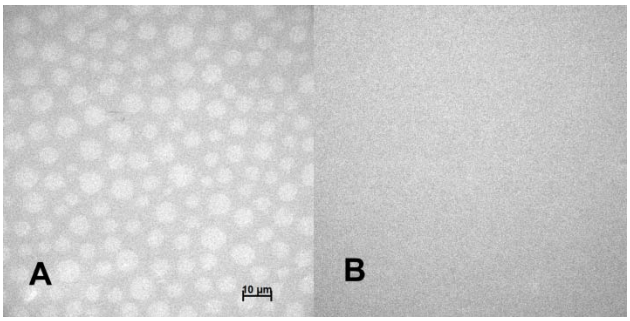

Figure S2: Representative EPI micrographs of NBD-DHPE distribution in an asymmetric bilayer containing Ml_o domains [LB composition: (2:1) (DOPC: CHOL); LS composition: (2.1:1.2:1.0) (DOPC: DPPC: CHOL)] (A) and a symmetric bilayer composition [LB and LS lipid composition: (1.5:0.5:1.0) DOPC: DPPC: CHOL] (B). In both bilayer systems, 5mol% of $diC_{18}M_{50}$ is included in the LB composition. The symmetric bilayer composition considers the hypothetical case, in which lipid flip flop would lead to the complete disappearance of the DOPC and DPPC concentration gradients across the bilayer.